

Resonance Tunneling in Double-Well Billiards with a Pointlike Scatterer

Taksu Cheon

Department of Physics, Hosei University, Fujimi, Chiyoda-ku, Tokyo 102, Japan

T. Shigehara

Computer Centre, University of Tokyo, Yayoi, Bunkyo-ku, Tokyo 113, Japan

(December 2, 1996)

The coherent tunneling phenomenon is investigated in rectangular billiards divided into two domains by a classically unclimbable potential barrier. We show that by placing a pointlike scatterer inside the billiard, we can control the occurrence and the rate of the resonance tunneling. The key role of the avoided crossing is stressed.

KEYWORDS: chaotic tunneling, quantum billiard, delta potential, diabolical degeneracy

3.65.-w, 4.30.Nk, 5.45.+b, 73.40.Gk

The tunneling is a quintessentially quantum phenomenon. However, with the path-integral formulation, a systematic semiclassical approximation can be formulated, and the problem can be treated in terms of the instanton, or the “classical orbit with imaginary time” in the region classically inaccessible [1]. One can assume, therefore, that the dynamics of this virtual classical orbits largely determines the characteristics of the tunneling phenomena. One can further conjecture that the tunneling in non-integrable system, with its chaotic virtual orbit, might display novel features unknown in the textbook examples of one-dimensional barrier penetration, or more generally, the tunneling in integrable systems [2,3]. Recent studies on several model systems show this is indeed the case. It has been revealed that very slight variation of the shape of the barrier can cause an unexpectedly large enhancement of the tunneling rate [4,5]. It is also found that the tunneling can be made arbitrary small by the proper choice of the shape parameter [6]. Certain evidence seems to link these characteristics to the chaotic character of the virtual classical trajectories [4,7–9]. At this point, however, there is no clear understanding about when and how the large variation in the tunneling rate occurs in non-integrable systems, and how this might be related to the chaos.

In this Letter, we start from the premise that we are still in need of a model which is rich enough to display all the essential features of the non-integrable tunneling, yet simple enough to allow the physical intuition to the phenomena. As a candidate for such a model, we propose a two-dimensional quantum billiard in which a particle moves around in a rectangular domain which is divided into two sub-domains by a finite-height barrier of rectangular shape parallel to the outer boundary. We further place a pointlike scatterer, or a Dirac’s delta potential in the domain on and off the barrier. We look at the change in the tunneling between two sub-domains while varying the location of the delta scatterer. This is intended as a “minimal model” for the change of the barrier shape. We show in the following that this model enables us to iden-

tify the key role of the diabolical points and avoided level crossing in the non-integrable tunneling. It also reveals the condition for the occurrence of the tunneling and its enhancement and suppression. The mirror symmetry of the system is shown *not* to be a necessary condition for the resonance tunneling.

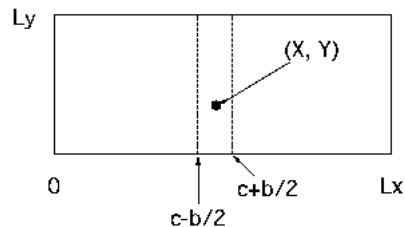


FIG. 1. A schematic depiction of the model billiard system. In the region $c-b/2 < x < c+b/2$, a potential barrier of height U_0 is placed. The pointlike scatterer located at (X, Y) is indicated by a filled circle.

We consider a quantum particle moving inside a rectangular hard wall of size $L_x \times L_y$ whose two sides are placed on the x and y axes. We put a barrier potential of constant height U_0

$$U(\vec{r}) = U_0 \theta(x_2 - x) \theta(x - x_1) \quad (1)$$

which divides the billiard into the left ($x < x_1$) and the right ($x > x_2$) sub-domains. We call the center and the width of the barrier c and b , so that we have $x_1 = c - b/2$ and $x_2 = c + b/2$. We then place a delta potential of strength v at $\vec{r} = \vec{R}$. The model is depicted in Fig. 1. Formally, the eigenvalue equation is

$$\left[-\frac{1}{2m} \nabla^2 + U(\vec{r}) + v \delta(\vec{r} - \vec{R}) \right] \psi_\alpha(\vec{r}) = \varepsilon_\alpha \psi_\alpha(\vec{r}). \quad (2)$$

It is known that this equation is meaningless as it stands [10]. However, the problem is known to be renormalizable with the introduction of the *formal* coupling \bar{v} in place of bare coupling v [10–13]. We write the eigenvalues and eigenstates for $\bar{v} = 0$ as η_n and ϕ_n , which we refer to

as unperturbed solutions. The full solution for $\bar{v} \neq 0$ is given in terms of the unperturbed basis. There are two kinds of solutions. The first, a trivial type of solution is

$$\varepsilon_\alpha = \eta_n \quad \text{if} \quad \phi_n(\vec{R}) = 0, \quad (3)$$

that is, if \vec{R} is on the node-line of the wavefunction $\phi_n(\vec{r})$. The second, more generic type of solution of eq. (2) is obtained from the equation

$$\overline{G}(\vec{R}; \varepsilon) - \frac{1}{\bar{v}} = 0 \quad (4)$$

where

$$\overline{G}(\vec{r}; \varepsilon) = \sum_n \phi_n(\vec{r})^2 \left[\frac{1}{\varepsilon - \eta_n} + \frac{\eta_n}{\eta_n^2 + 1} \right] \quad (5)$$

is the renormalized Green's function. The eigenfunction corresponding to the eigenvalue ε_α is given by

$$\psi_\alpha(\vec{r}) = \sum_n \frac{\phi_n(\vec{R})}{\varepsilon_\alpha - \eta_n} \phi_n(\vec{r}). \quad (6)$$

We first consider the case in which the system has mirror symmetry with respect to the $x = L_x/2$ line which divides the billiard evenly to left and right domains. For this, we place the barrier at the center, $c = L_x/2$, and also locate the pointlike scatterer along $x = L_x/2$ line, namely $X = L_x/2$. Because of the mirror symmetry, the eigenfunction of the system possesses definite parities. When U_0 is sufficiently large, there are nearly degenerate parity doublets $(\psi_{\alpha-}, \psi_{\alpha+}) \equiv (\psi_\alpha, \psi_{\alpha+1})$ with energies $(\varepsilon_{\alpha-}, \varepsilon_{\alpha+}) \equiv (\varepsilon_\alpha, \varepsilon_{\alpha+1})$ where we assume α to be an odd integer. From these parity doublets, one can construct the wave functions

$$\chi_\alpha^{(\pm)} \approx \frac{1}{\sqrt{2}} (\psi_{\alpha-} \pm \psi_{\alpha+}) \quad (7)$$

which are localized to opposite sub-domains. The localized states in each sub-domain $\chi_\alpha^{(\pm)}$ evolve according to

$$e^{iHt} \chi_\alpha^{(\pm)} \approx \exp(i\bar{\varepsilon}_\alpha t) \left(\chi_\alpha^{(\pm)} \cos\left(\frac{\Delta_\alpha t}{2}\right) - i\chi_\alpha^{(\mp)} \sin\left(\frac{\Delta_\alpha t}{2}\right) \right) \quad (8)$$

where

$$\bar{\varepsilon}_\alpha \equiv \frac{\varepsilon_{\alpha+} + \varepsilon_{\alpha-}}{2} \quad \text{and} \quad \Delta_\alpha \equiv \varepsilon_{\alpha+} - \varepsilon_{\alpha-} \quad (9)$$

are the average energy and the energy splitting of the parity doublet $\psi_{\alpha-}$ and $\psi_{\alpha+}$. This means that the system oscillates between the states $\chi_\alpha^{(+)}$ and $\chi_\alpha^{(-)}$ with the half period $T = \pi/\Delta_\alpha$. This is a quantum beating, or a resonance tunneling between two nearly degenerate states. The rate of the tunneling between the left and the right domains D_α is given by

$$D_\alpha \equiv \frac{1}{T} = \frac{1}{\pi} \Delta_\alpha. \quad (10)$$

Therefore, the energy splitting of the parity doublet Δ_α is a direct measure of the tunneling rate.

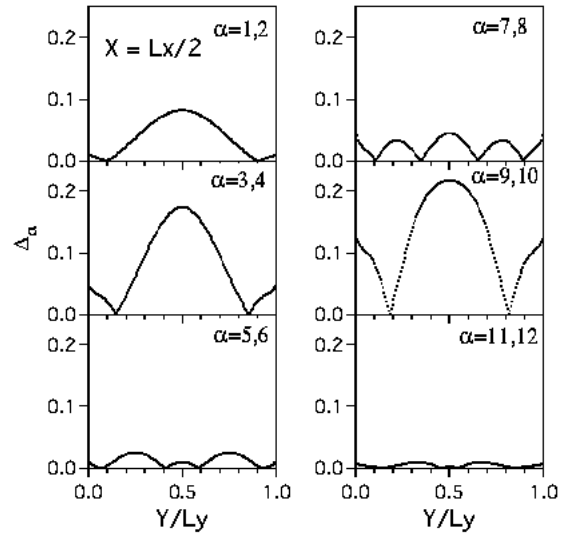


FIG. 2. The energy splitting of the parity doublets as the function of perpendicular location of the pointlike scatterer. Its horizontal location is kept at the middle $X = L_x/2$. The parameters are chosen as $L_x = 1.618$, $L_y = 1/L_x$, $U_0 = 50$, $c = L_x/2$, $b = L_x/10$ and $\bar{v} = 100$.

Because of the two dimensional nature of our model system, there is still a freedom to choose the perpendicular location of the pointlike scatterer, Y . We look at the Y -dependence of the energy splitting of the parity doublets. In Fig. 2, a specific example of $L_x = (\sqrt{5} + 1)/2$, $L_y = 1/L_x$, $b = L_x/10$ and $U_0 = 50$ is shown. The mass of the system is chosen to be $m = 2\pi$, and the formal coupling is set to $\bar{v} = 100$. With this choice of \bar{v} , the states near the ground state come into the strong coupling region [13]. Most notable feature in the Figure is the fact that at certain values of Y , the energy splitting, thus the tunneling rate is enhanced by several times compared to the unperturbed case, which, in the Figure, is seen as $Y = 0$ and $Y = L_y$. Another point, no less important, is that there are several values of Y in which the energy splitting becomes zero. This means that even with finite height potential, one can totally suppress the tunneling by positioning the pointlike scatterer appropriately. Since the Green's function $\overline{G}(\vec{R}, \varepsilon)$, eq. (5) is a monotonously decreasing function of ε except at its poles, eq. (4) cannot have degenerate solutions. The zero splitting of two energy eigenstates can occur only as the joint solution of eqs. (3) and (4). Therefore, the location of the pointlike scatterer \vec{R}^* at which the total suppression of the resonance tunneling occurs is determined by [14]

$$\phi_n(\vec{R}^*) = \overline{G}(\vec{R}^*, \eta_n) - \frac{1}{\bar{v}} = 0. \quad (11)$$

Since \vec{R} is a two dimensional vector, the solution of eq. (11) are the isolated points. These points are known as

the *diabolical points* which play central role in the phenomena of Berry phase [15].

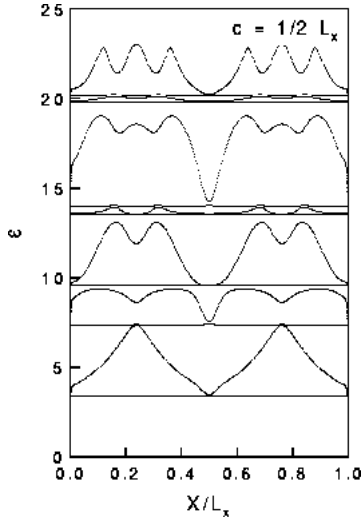


FIG. 3. First fourteen eigenvalues as the function of horizontal location of the pointlike scatterer. The perpendicular location is fixed at $Y = 0.4142L_y$. See Fig. 2 for the values of parameters. The values $X = 0$ and L_x correspond to no pointlike scatterer.

Next, we let the horizontal location of the pointlike scatterer X to vary. In Fig. 3, we show the first fourteen eigenvalues as a function of X while fixing the Y at $(\sqrt{2} - 1)L_y$. One observes that two levels approach to each other not only at $X = L_x/2$, but also at other places. Indeed, The solution of eq. (11) needs not to be restricted to the line $x = L_x/2$: It can be on any nodeline $\phi_n(\vec{r}) = 0$ of the relevant unperturbed wave function. Examples are shown in Fig. 4, where we mark the diabolical locations with asterisks for several eigenstates. When the pointlike scatterer is at the diabolical locations, any combination of degenerate states can be chosen as the eigenstate. One can form two eigenstates which cross over the barrier to have equal amount of probability distribution in left and right sub-domains with opposite relative signs at one sub-domain. This is a generalization of the parity doublet states for the mirror symmetric system. The doublet states with equally partitioned wave function remain to be the eigenfunction of the system if the pointlike scatterer is moved off the diabolical location in the direction parallel to the y -axis along the nodeline $\phi_n(\vec{r}) = 0$. This is understood if one notices that one of the unperturbed states remains to be the full eigenstate. When the pointlike scatterer is not on the nodeline, the eigenstates are localized either to the left or the right sub-domains. The numerical example in Fig. 4, which depicts the parameter space (X, Y) , illustrates the situation. When the pointlike scatterer is placed at shaded region, the α -th eigenstate is localized at the right sub-domain, and when at unshaded region, localized at the left. The figure is drawn by defining an

index

$$l_\alpha = \int_0^{x_d} dx \int_0^{L_y} dy \psi_\alpha^*(x, y) \psi_\alpha(x, y) \quad (12)$$

with x_d signifying the location of the central nodeline of “odd” unperturbed wavefunction. Typically, x_d is close to the center of the barrier, namely, $x_d \simeq c$. The shade indicates the region where l_α exceeds 1/2. It is on the line of $l_\alpha = 1/2$ which separates the shaded and unshaded regions where the resonance tunneling can occur. This example clearly shows that it is not the mirror symmetry of the problem that brings the resonance tunneling phenomenon, but rather the existence of the crossover between the two wave functions with opposite localization characteristics [16].

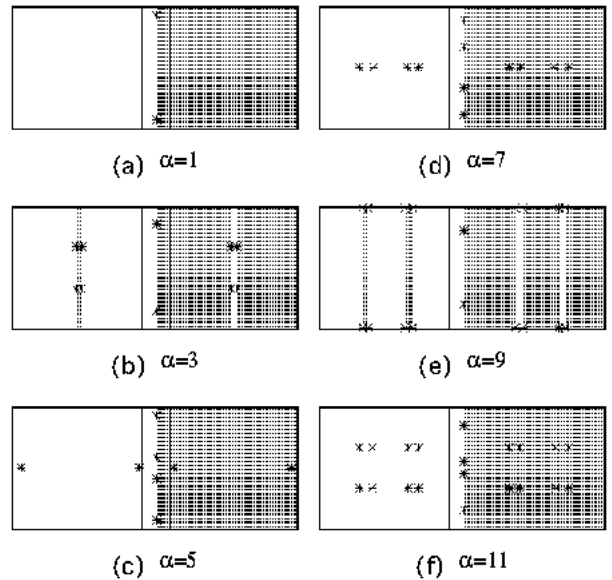


FIG. 4. This chart shows the parameter space (X, Y) with the localization status of the α -th eigen function. The shaded area represents the location of the pointlike scatterer at which the localization index l_α is more than 1/2. The asterisks are the diabolical locations. The resonance tunneling occurs near the interface of shaded and unshaded areas. The barrier is placed at the middle ($c = L_x/2$). Other parameters are also chosen as in Fig. 2.

We now consider the more generic case in which the mirror symmetry is broken in the unperturbed level. As an example, we place the barrier of height $U_0 = 50$ and width $b = 1/10 \times L_x$ at slightly left of the middle $c = 19/40 \times L_x$. We thus have $x_1 = 17/40 \times L_x$ and $x_2 = 21/40 \times L_x$. Other parameters are kept to be same as before. The unperturbed states again form the doublets $\{\phi_\alpha, \phi_{\alpha+1}\}$ (α : odd). But the states ϕ_α and $\phi_{\alpha+1}$ are localized in the opposite side of the barrier. Therefore, no resonance tunneling can be observed in the unperturbed system. We proceed to place the pointlike scatterer of strength $\bar{v} = 100$ at the location (X, Y) . In Fig. 5,

we show the first fourteen eigenvalues as a function of X with a fixed value for Y . ($Y = (\sqrt{2} - 1)L_y$ in this example.) One can spot several avoided level crossings. Specifically, the ones near $X = L_x/2$ appear to separate the two distinct regions of the parameter space.

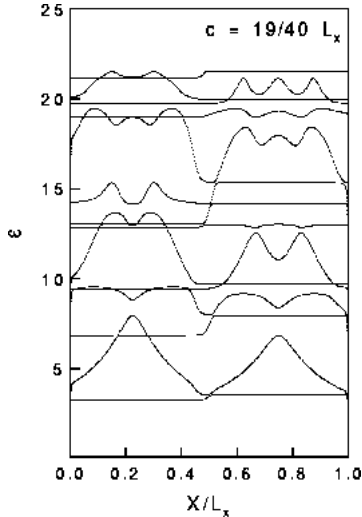


FIG. 5. Same as Fig. 3 except that the barrier is slightly shifted leftward ($c = 19/40L_x$).

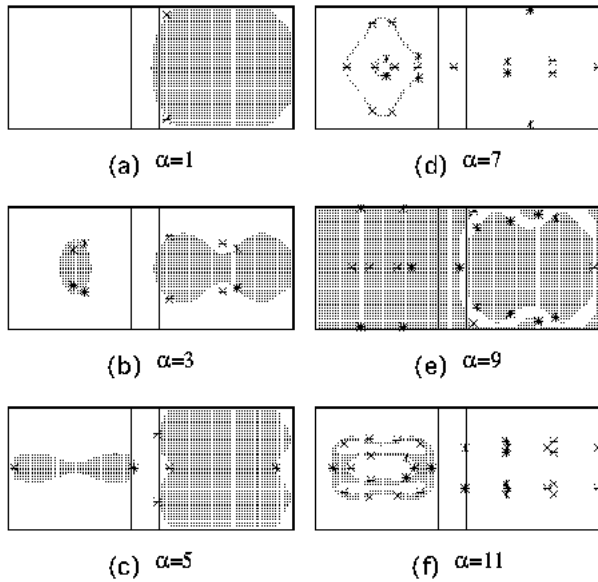


FIG. 6. Same as Fig. 4 except that the barrier is slightly shifted leftward ($c = 19/40L_x$).

In Fig. 6, the parameter space (X, Y) is depicted with diabolical points (asterisks) and localization characteristics (shades) in an analogous manner as in Fig. 4. Namely, when the pointlike scatterer is placed at shaded region, the α -th eigenstate is localized at the right subdomain, and when at unshaded region, localized at the left. The line of resonance tunneling on which $l_\alpha = 1/2$ now becomes the closed loops which separate the regions

into left and right localization. The resonance tunneling can occur only when \vec{R} is located very close to this loop. When one moves the pointlike scatterer along the loop, the rate of the tunneling goes through a variation. The rate becomes zero at the diabolical points, and the maximum values tends to come at the points on the loop in between the diabolical points in a manner similar to the one found in Fig. 2. We conclude that the mirror symmetry is not essential to obtain the resonance tunneling in double-well billiards.

The mechanism behind the localization structure shown in Fig. 6 can be further elucidated by a closer inspection of the energy level diagram around the avoided crossing region. There, we can assume that considering the mixing of two levels is sufficient. For the unperturbed doublet $\{\phi_\alpha, \phi_{\alpha+1}\}$ of opposite localization properties, we can approximate eqs.(4) and (5) as

$$\frac{\phi_\alpha(\vec{R})^2}{\varepsilon - \eta_\alpha} + \frac{\phi_{\alpha+1}(\vec{R})^2}{\varepsilon - \eta_{\alpha+1}} = \frac{1}{v_{\text{eff}}} \quad (13)$$

where we define

$$\frac{1}{v_{\text{eff}}} \equiv \frac{1}{\bar{v}} - \sum_{n \neq \alpha, \alpha+1} \phi_n(\vec{R})^2 \left(\frac{1}{\frac{(\eta_\alpha + \eta_{\alpha+1})}{2} - \eta_n} + \frac{\eta_n}{\eta_n^2 + 1} \right) - \phi_\alpha(\vec{R})^2 \frac{\eta_\alpha}{\eta_\alpha^2 + 1} - \phi_{\alpha+1}(\vec{R})^2 \frac{\eta_{\alpha+1}}{\eta_{\alpha+1}^2 + 1}. \quad (14)$$

Here, we have replaced the energy ε in all terms other than $n = \alpha$ and $n = \alpha + 1$ by $(\eta_\alpha + \eta_{\alpha+1})/2$. The quantity v_{eff} is a function of both α and \vec{R} . The solution of eq. (13) is readily obtained as

$$\varepsilon_{\alpha\pm} = \frac{(\eta_\alpha + \eta_{\alpha+1})}{2} + \frac{v_{\text{eff}}(f_\alpha + f_{\alpha+1})}{2} \pm \frac{1}{2} \sqrt{\{(\eta_{\alpha+1} - \eta_\alpha + v_{\text{eff}}(f_{\alpha+1} - f_\alpha))^2 + 4v_{\text{eff}}^2 f_\alpha f_{\alpha+1}\}}. \quad (15)$$

where we have used the notation $f_\alpha \equiv \phi_\alpha(\vec{R})^2$. The corresponding eigenfunctions are given, apart from the normalization, by

$$\psi_{\alpha\pm}(\vec{r}) \propto \frac{\phi_\alpha(\vec{R})}{\varepsilon_{\alpha\pm} - \eta_\alpha} \phi_\alpha(\vec{r}) + \frac{\phi_{\alpha+1}(\vec{R})}{\varepsilon_{\alpha\pm} - \eta_{\alpha+1}} \phi_{\alpha+1}(\vec{r}). \quad (16)$$

Along a path of varying \vec{R} (for example, along the line $Y = \text{constant}$ as in Fig. 5), the avoided crossing takes place at the minimum value of the energy splitting $|\varepsilon_{\alpha+} - \varepsilon_{\alpha-}|$. This occurs when we have

$$\phi_\alpha(\vec{R})^2 \gg \phi_{\alpha+1}(\vec{R})^2 \quad \text{and} \quad \frac{1}{v_{\text{eff}}} = \frac{\phi_\alpha(\vec{R})^2}{\eta_{\alpha+1} - \eta_\alpha} \quad (17a)$$

for the case of $v_{\text{eff}} > 0$, and when

$$\phi_\alpha(\vec{R})^2 \ll \phi_{\alpha+1}(\vec{R})^2 \quad \text{and} \quad \frac{1}{v_{\text{eff}}} = -\frac{\phi_{\alpha+1}(\vec{R})^2}{\eta_{\alpha+1} - \eta_\alpha} \quad (17b)$$

for $v_{\text{eff}} < 0$. We consider the case of (a). Analogous argument can be made for case (b). Inserting the second condition of eq.(17a) into eq. (15), we obtain

$$\varepsilon_{\alpha\pm} = \frac{\eta_{\alpha} + \eta_{\alpha+1}}{2} + \frac{\eta_{\alpha+1} - \eta_{\alpha}}{2} \left(1 + \gamma^2 \pm \gamma\sqrt{4 + \gamma^2}\right) \quad (18)$$

where we use the notation $\gamma \equiv |\phi_{\alpha+1}(\vec{R})/\phi_{\alpha}(\vec{R})|$. The ratio between the two components of $\psi_{\alpha\pm}(\vec{r})$ in eq. (16) is given by

$$\left| \frac{\phi_{\alpha+1}(\vec{R})/\phi_{\alpha}(\vec{R})}{\varepsilon_{\alpha\pm} - \eta_{\alpha+1}} \right| = \left| \frac{2}{\gamma \pm \sqrt{4 + \gamma^2}} + \gamma \right| \quad (19)$$

Because we have $\gamma \simeq 0$ (the first condition of eq. (17a)), this ratio becomes very close to 1, giving one-to-one mixing of the states of opposite localization properties. We can conclude that the resonance tunneling occurs at the parameter values corresponding to the avoided crossing. Therefore, in the whole parameter space (X, Y) , the line of resonance tunneling is the ‘‘valley line’’ of minima of the energy splitting $|\varepsilon_{\alpha+} - \varepsilon_{\alpha-}|$. At the diabolical points, γ becomes exactly zero. We also observe from eq. (18), that both levels are close to the unperturbed level $\varepsilon = \eta_{\alpha+1}$ at the avoided crossing. (This becomes $\varepsilon = \eta_{\alpha}$ for $v_{\text{eff}} < 0$ case.) These features are exactly what one finds in the numerical example of Figs. 5 and 6.

Finally, we discuss our results in a broader view. The role of the diabolical points in the resonance tunneling has been already recognized by the authors of refs. [6] and [7]. The clarification of its distribution in the parameter space and its decisive role in shaping the line of resonance tunneling is made possible only with the very simple setting of the current work. Although the model studied here is a simplistic one, we can conjecture that our main finding is applicable to generic non-integrable tunneling systems: The resonance tunneling occurs along the ‘‘valley line’’ of avoided crossing in the parameter space of the barrier shape, and the rate of tunneling undergoes a large variation when the shape parameters go through the diabolical points.

In the current study, we have made no immediate reference to chaotic motion nor to the semiclassical analysis, since the system is solvable in full quantum mechanical setting. However, if we look at the doublet states in higher energy with higher number of nodes, we expect the appearance of complex pattern both in the distribution of the diabolical locations and in the shape of the line on which resonance tunneling takes place. One can also make the tunneling more complex in above sense by placing more than one pointlike scatterers in the billiards. The semiclassical approach to such problem will be an interesting and challenging task.

It is known that the effect of the pointlike scatterer disappears in the classical limit [14]. The fact that the classically non-observable object causes the large change

in the tunneling rate is a good example showing the intricacy of the quantum physics. We also stress that the system considered here is not just of academic nature, but may actually be tested either through quantum dot or through microwave experiments. Even its application as a switching device in the nanometer scale might be speculated as a remote possibility.

In summary, we have studied several characteristics of non-integrable tunneling phenomena through the numerical examples of a double-well billiard with a pointlike scatterer. We have identified the key role of the diabolical crossings in the tunneling.

We acknowledge the helpful discussion with the members of the theory division of Institute for Nuclear Study, University of Tokyo.

-
- [1] S. Coleman, *Aspects of Symmetry* (Cambridge University Press, Cambridge, 1985).
 - [2] M Wilkinson, *Physica* **D21** (1986) 341.
 - [3] S. C. Creagh, *J. Phys.* **A27** (1994) 4969.
 - [4] O. Bohigas, S. Tomsovic and D. Ullmo, *Phys. Rev. Lett.* **65** (1990) 5.
 - [5] W. A. Lin and L. E. Ballentine, *Phys. Rev. Lett.* **65** (1990) 2927.
 - [6] F. Grossmann, T. Dittrich, P. Jung and P. Hänggi, *Phys. Rev. Lett.* **67** (1991) 516.
 - [7] S. Tomsovic and D. Ullmo, *Phys. Rev.* **E50** (1994) 145.
 - [8] A. Shudo and K. S. Ikeda, *Phys. Rev. Lett.* **74** (1995) 682.
 - [9] S. C. Creagh and N. D. Whelan, LANL preprint chaodyn/9608002.
 - [10] S. Albeverio, F. Gesztesy, R. Høegh-Krohn and H. Holden, *Solvable Models in Quantum Mechanics* (Springer-Verlag, New York, 1988).
 - [11] P. Šeba, *Phys. Rev. Lett.* **64** (1990) 1855.
 - [12] T. Shigehara, *Phys. Rev.* **E50** (1994) 4357.
 - [13] T. Shigehara and T. Cheon, *Phys. Rev.* **E54** (1996) 1321.
 - [14] T. Cheon and T. Shigehara, *Phys. Rev. Lett.* **76** (1996) 1770.
 - [15] M. V. Berry, *Proc. Roy. Soc. Lond.* **A392** (1984) 43.
 - [16] A. Peres, *Phys. Rev. Lett.* **67** (1991) 158.
 - [17] M. V. Berry, *Proc. Roy. Soc. London* **422** (1989) 7.